

# Frequency-Dependent Cohesive Zone Models for Fatigue

S Salih, K Davey, Z Zou

School of Mechanical, Aerospace and Civil Engineering, The University of Manchester  
eng.sarmed@gmail.com

**Abstract:** This paper is concerned with a new cohesive zone model (CZM) to better describe the effects of rate and cyclic loading. Rate is known to affect the manner in which cracks propagate in materials, yet there presently exists no rate-dependent cohesive model for fatigue simulation. The frequency of the applied cyclic load is recognised to influence crack growth rates with crack growth significantly different at lower frequencies due to microstructural effects or other damage mechanisms such as creep or corrosion. A rate-dependent trapezoidal cohesive model is presented that has the ability to capture this behaviour and shows slower rates of crack propagation with higher loading frequencies. This is achieved by allowing the cohesive fracture energy to increase with frequency up to a specified limit. On unloading the cohesive model retains material separation, which accumulates with the number of loading cycles, leading to final failure. An experimental fatigue investigation is currently underway to validate the new cohesive model, which has been coded in a UMAT subroutine and implemented in ABAQUS.

**Keywords:** Cohesive zone model; Rate effect; Fatigue; Frequency effect; Rate-dependent CZM

## 1. Introduction

The process of fatigue failure can be divided into three parts: crack initiation, crack propagation, and then fast fracture, which leads ultimately to the final failure [1], [2]. Fatigue can be classified as a subcritical failure mechanism, occurring when the applied stress is significantly lower than the yield stress of the material. Mechanical, microstructural and environmental factors can significantly influence the fatigue behaviour of a part. Consequently fatigue analysis is primarily an empirical study founded on extensive experimental investigations typically needed to evaluate and understand material behaviour and estimate the life of mechanical parts. These can be costly and extremely time-consuming giving rise to an urgent requirement for fatigue models possessing an ability to predict crack growth rates and fatigue life [2].

The limitation of conventional fatigue models has heightened the need for a model that is applicable at crack initiation, as well as for crack growth. Hence, the recent focus on cohesive zone models (CZMs), which were initially advanced by Dugdale [3] and Barenblatt [4] in order to overcome the unrealistic mathematical-stress singularity at a crack tip [5]. In Dugdale's model the stress in the small plastic zone ahead of the crack tip is finite and equal to the yield strength, while in Barenblatt's model the stress in the region in front of the crack is a function of the ligament length. The CZM became more popular following the work of Hillerborg et al. [6], which demonstrated that numerical analysis was possible using the finite element method and a bilinear cohesive zone model (BCZM).

The CZM is founded on a traction-separation law (TSL), where traction is related to material separation through a constitutive equation. On traction reaching a critical value  $\sigma_c$ , material damage initiates and material softening occurs. Following damage initiation, traction decreases until it finally reaches zero which is the point of material separation. This point is also identified by the separation between the surfaces of the cracked material attaining a critical value  $\delta_c$ ; at this point all cohesive energy  $\Gamma_0$  has been dissipated and consequently the crack propagates. The advantage of using a cohesive model over other



models is its ability to predict the initiation and the propagation of cracks along with its applicability to monotonic and cyclic loading.

It is well appreciated that cyclic loading presents added complication arising out of the unloading part of the loading cycle and the history dependence of the fatigue process. Most conventional CZMs are limited to monotonic crack growth prediction; see for example the models of: Needleman [7], Needleman [8], Scheider [5] and Tvergaard & Hutchinson [9], which are reversible and history-independent. There exists irreversible models such as those presented in references [10]–[13], but these are history-independent and do not include a mechanism to cater for cyclic-damage accumulation. These are consequently limited to the simulation of monotonic-crack propagation. A CZM for fatigue requires an irreversible and history-dependent cohesive law, which is needed to capture the damage accumulation associated with loading-unloading hysteresis. This is a feature of the model introduced by De-Andrés et al. [14], which involves a damage factor  $D$  that represents the value of dissipated energy in the fracture process divided by the critical fracture energy. Dahlan [2] adopted a similar damage concept involving a variable that cumulatively recorded the value of the separation at the end of each loading cycle with failure identified by the accumulated value reaching  $\delta_c$ . A different damage accumulation mechanism has been used in [15], involving a degrading cohesive stiffness with damage accumulation. Two stiffness parameters ( $K^+$  and  $K^-$ ) are used for loading and unloading, where the value of  $K^-$  is constant for each unloading, but  $K^+$  is allowed to evolve with the number of cycles through a decay factor, until the complete separation of the cohesive element. An adapted Paris-like equation is used, where fatigue crack growth rate  $da/dN$  is related to the change in crack tip opening displacement range per cycle  $\Delta\delta$  as in the equation  $da/dN = C(\Delta\delta)^n$ . However, the use of  $\Delta\delta$  as a material property is questionable as it depends to some extent on the degree of mechanical constraint [16]. A similar but slightly different approach was adopted by Yang et al. [17], with a model also involving loading and the unloading stiffness parameters but in this case both are functions of a damage parameter that evolves during loading and unloading cycles. A recent study by Roe & Siegmund [16] investigated a CZM with a degrading cohesive strength as a function of the damage; the model involves two additional parameters, i.e.  $\sigma_f$ , which is the endurance limit and  $\delta_\Sigma$ , which is the accumulated cohesive length. In this model, if the stress on the element ahead of the crack tip is less than the endurance limit, then the model will present infinite life (i.e. no crack propagation). If the stress is larger than the endurance limit, then material separation accumulates until it reaches the cohesive length  $\delta_o$ , which represents separation at the critical cohesive stress  $\sigma_c$ . Subsequently on reaching  $\delta_o$ , damage accumulates and the critical cohesive stress reduces as a function of the damage; the crack extends and the cohesive element fails when the maximum value of the stress in the loading cycle reaches the current critical cohesive stress. Other studies [18], [19] have considered relatively similar approaches, in which the damage will not accumulate if the stress is less than a predefined value (i.e. an endurance limit). All the methods mentioned above are rate-independent models and do not capture the frequency effect. In this study a trapezoidal rate-dependent CZM introduced by Salih et al. [13] is further developed to be used for the simulation of the fatigue crack growth.

## 2. Cohesive zone model for fatigue

Different types of TSL are presented in the literature, which include the: polynomial, exponential, bilinear, and trapezoidal as shown in Figure 1. The CZM is recognised not to be a physical material model but a phenomenological law that is designed to capture the essence of the fracture process. Therefore, there is no underpinning physical evidence to support a particular shape of the curve that describes the relationship between traction and separation. In this study the Trapezoidal TSL has been used because of its ability to capture plasticity locally.

The behaviour of the existing model introduced by Salih et al. [13] is best understood and described by an arrangement of 1-D spring, slider, dashpots, and linear cohesive elements as depicted in Figure 2. Rate dependency is recognised to arise from the behaviour of the dashpots. In this work a frequency-

dependent cohesive zone model for fatigue is produced in a similar manner, but in this model the critical stress increases as a function of the loading frequency and the increase in the frequency-dependent critical cohesive stress is automatically limited by the rate equation. The traction-separation curve for this model is shown in Figure 3.

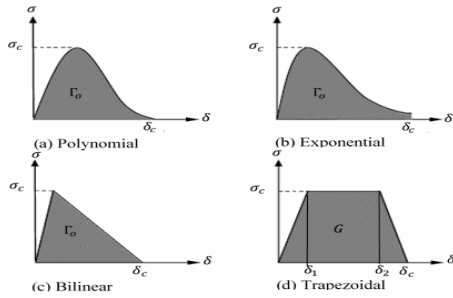


**Figure 1.** Common traction-separation

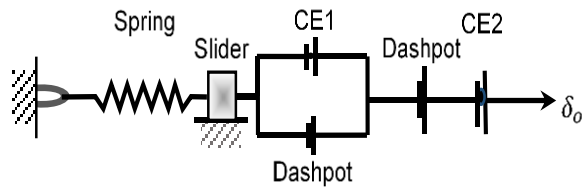


**Figure 2.** Mode I Cohesive Zone model

The area under the traction separation curve represents the fracture energy  $G_c$ , which is defined mathematically to be

$$G_c = \int_0^{\delta_c} \sigma(\delta) d\delta \quad (1)$$

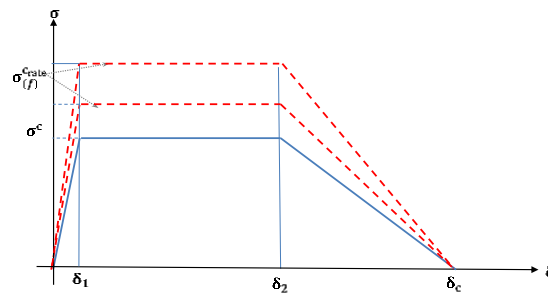


**Figure 3.** Mode I Cohesive Zone model

In the case of trapezoidal CZM the fracture energy can be considered to be formed in two parts, i.e. plastic  $G_p$  and cohesive  $\Gamma_0$  components to give

$$G_c = G_p + \Gamma_0 \quad (2)$$

The area under the curve(s) in Figure 3 is equal to

$$G_c = \frac{1}{2} \sigma_c^{rate} ((\delta_2 - \delta_1) + \delta_c) \quad (3)$$

$$\sigma_{(f)}^{rate} = \sigma_c \begin{cases} 1 & \text{if } f \leq 0.05 \\ (0.52 + \frac{1}{a+b \exp(-((\frac{d*(f-f_{min})}{f_{min}})^n)))} & \text{if } f > 0.05 \end{cases} \quad (4)$$

The meanings the symbols relay are:  $G_c$  is the total dissipated energy per unit area,  $G_p$  is the local plastic dissipated energy,  $\Gamma_0$  is the energy dissipated in the formation of new surfaces,  $\sigma_{(f)}^{rate}$  is the frequency-dependent critical cohesive traction,  $\sigma_c$  is the rate-independent critical cohesive traction,  $\delta_1$  is the displacement when the traction first reach its critical value,  $\delta_2$  is the displacement at which the element deterioration is assumed to start, and  $\delta_c$  is the rate-independent critical cohesive separation.  $a$ ,  $b$ ,  $d$  and  $n$  are fixed and are determined with experimental data; a first estimation of these constants is: 1.2, 0.85, 3 and 0.25. The lowest frequency  $f_{min}$  is equal to 0.05Hz,  $f$  is the applied frequency and

$$\delta_2 \leq 0.75 \times \delta_c \quad (5)$$

The monotonic trapezoidal TSL depicted in Figure 3 is represented mathematically as

$$\sigma(\delta) = \sigma_{(f)}^{c_{rate}} \begin{cases} \frac{\delta}{\delta_1} & \text{if } 0 < \delta < \delta_1 \\ 1 & \text{if } \delta_1 \leq \delta \leq \delta_2 \\ (1 - D) & \text{if } \delta_2 < \delta < \delta_c \end{cases} \quad (6)$$

In the cohesive model the mechanism of crack propagation is void nucleation, growth and coalescence. The damage variable ( $D$ ) can be understood to be the ratio between damaged area ( $A_d$ ) (the accumulated areas of the voids) to undamaged reference area ( $A_e$ ) [20]. In the present configuration damage can be represented by the relationship

$$D = \frac{A_d}{A_e} = \frac{\delta - \delta_2}{\delta_c - \delta_2} \quad (7)$$

Unloading and subsequent reloading occurs at a constant stiffness  $K = \sigma_{max}/\delta_{max}$ , where  $\sigma_{max}$  and  $\delta_{max}$  are the stress and the separation at the point where unloading starts, respectively. In this case traction is evaluated by

$$\sigma(\delta) = K \times \delta \quad (8)$$

The cohesive model described thus far, will result in an infinite life when cyclic load is applied. So in order to capture finite life, it is necessary to use an irreversible and history dependent cohesive zone model. This can be done by identifying a damage variable that accumulates with the number of cycles. The damage mechanism in this model consists of two parts: first is the remnant plastic separation ( $\delta^p$ ), which accumulates as a result of cyclic plasticity, and second the damage variable  $D$  that represents the material deterioration in the CZM. The proposed damage accumulation mechanism is designed to provide the trapezoidal model with an ability to capture fatigue crack growth. A full mathematical description of the proposed new model is:

$$\sigma(\delta) = \sigma_{max} \begin{cases} \left( \frac{\delta_{eff}}{\delta_{max} - \delta^p} \right) & \text{if } \delta_{eff} < 0 \\ \left( \frac{\delta_{eff}}{\delta_{max} - \delta^p} \right) H_{(\delta_{eff} - \delta^p)} & \text{if } 0 \leq \delta_{eff} \leq \delta_{max} \\ 1 & \text{if } \delta_{max} < \delta_{eff} \leq \delta_2 \\ (1 - D) \times \frac{\sigma_{(f)}^{c_{rate}}}{\sigma_{max}} & \text{if } \delta_2 < \delta_{max} < \delta_{eff} < \delta_c \\ 0 & \text{if } \delta_{eff} \geq \delta_c \end{cases} \quad (9)$$

where  $\sigma_{max}$  and  $\delta_{max}$  are the stress and the separation at the end of the loading cycle respectively, but at the beginning when there is no unloading these values set to be equal to  $\sigma_{(f)}^{c_{rate}}$  and  $\delta_1$ , respectively.

The parameter  $\delta^p$  records the value of the remnant separation at the end of the loading cycle. This is required because at unloading, separation does not return to zero. The Heaviside function  $H_{(\delta_{eff} - \delta^p)}$  equals zero if  $\delta_{eff}$  is smaller than  $\delta^p$  and one in other cases and finally  $D$  is a damage variable of equation (9) with  $\delta_{eff}$  replacing  $\delta$ . In addition

$$\delta_{eff} = \delta^{cyc} + \delta^p \quad (10)$$

$$\delta_{(i+1)}^p = \delta_{(i)}^p + \frac{\delta_{max}^{cyc}}{C} \quad (11)$$

where  $\delta^{cyc}$  and  $\delta^p$  are the cyclic applied displacement and the stored plastic displacement respectively. The material parameter  $C$  dictates the level of cyclic plasticity and its value is determined on tuning the analysis results to fit with the experimental data.

In this model, the value of the stored separation ( $\delta^p$ ) accumulates with increasing number of loading cycles until it reaches  $\delta_2$  at which point material softening begins and the cohesive element fails when the effective separation (the accumulated plus the cyclic) reaches the critical cohesive separation  $\delta_c$ . Figure 4 shows the behaviour of the cohesive model under monotonic and cyclic loads.

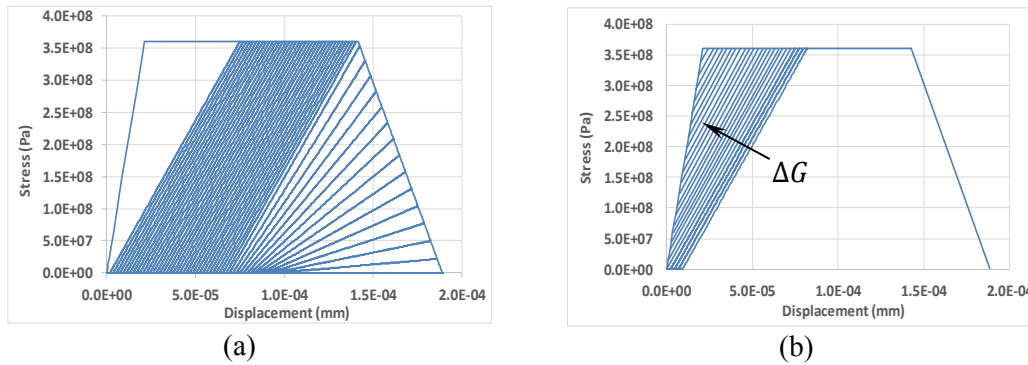


**Figure 4.** Behaviour of the cohesive model: (a) cyclic loads, (b) cyclic-dissipated energy

The accumulated dissipated energy ( $\Delta G$ ) as shown in Figure 4b can be calculated by:

$$\Delta G = \begin{cases} \frac{1}{2} \left[ \sigma_{(f)}^{rate} (\delta_{max} + \delta^p - \delta_1) \right] & \text{if } \delta_{max} \leq \delta_2 \\ \frac{1}{2} \left[ \sigma_{(f)}^{rate} (\delta_{max} + \delta_2 - \delta_1) + \sigma_{max} (\delta^p - \delta_2) \right] & \text{if } \delta_{max} > \delta_2 \end{cases} \quad (12)$$

From the analysis is found that a minimum number of 20 elements in the cohesive zone should be used to obtain satisfactory results, although in this study higher numbers were used in order to have superior control of the crack growth. The length ( $l_{coh}$ ) can be estimated through a similar formula used for the plastic zone evaluated by von Mises yield criterion, i.e.

$$l_{coh} = \frac{E}{2\pi} \frac{G_{Ic}}{\sigma_c^2} \quad (13)$$

### 3. Implementation of the cohesive zone model in abaqus

Numerical analysis is performed using the commercial finite element solver ABAQUS. Although a cohesive element exists in ABAQUS, the traction separation laws associated with this element are history independent and cannot be used for the simulation of the fatigue problem. The CZM described in Section 2 has been incorporated into ABAQUS through a user defined material subroutine UMAT. This subroutine provides the user with a facility to identify a specific constitutive behaviour and link this behaviour to any element.

#### 3.1. Implementing and testing the UMAT

To test the UMAT, a model that consists of two material elements and one cohesive element connecting them was used as shown in Figure 5. The material properties were set to be elastic in the bulk material elements with 192 GPa for the elastic modulus and 0.29 Poisson's ratio, while the cohesive element set to have a critical stress of 360 MPa, critical separation of 0.189 mm and 17000 GPa elastic stiffness. The value of the parameter  $C$  is set to a small value (20) in order to artificially reduce the number of cycles required for the cohesive element to fail. The cyclic stress is shown in Figure 4a with respect to the separation and in Figure 6 with respect to the time. The figures show how the plastic separation is accumulating with the number of cycles until the accumulated plus the applied separation reaches  $\delta_2$ . Subsequently the cohesive stiffness decreases with the number of cycles as a consequence of material deterioration and the cohesive element fails when the stress reaches zero.



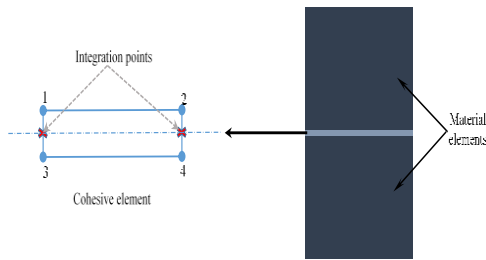


**Figure 5.** Implementation of the CE in the FE model

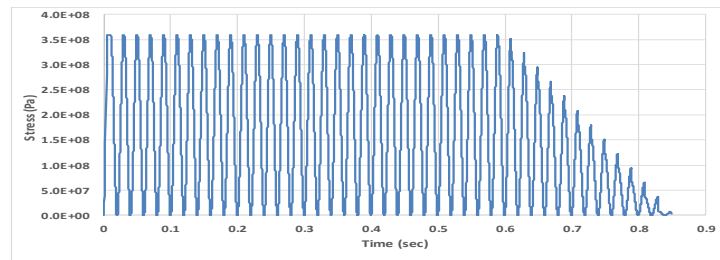


**Figure 6.** Stress levels in the cohesive element

### 3.2. Analysis model: geometry and boundary conditions

The finite element model used in this work is shown in Figure 7. The model consists of 23621 plane-stress elements of which 22991 (type CPS4) and 390 (type CPS3), and 240 cohesive elements (type COH2D4) [21]. In the commercial finite element solver ABAQUS, the cohesive behaviour can be identified either as a cohesive surface or by implementing cohesive elements along the crack path; these cohesive elements adjoin with the bulk material elements. In this study, the second method has been used, since in this method the cohesive behaviour is defined through the material behaviour attributed to those elements. A mesh sensitivity analysis has been performed which confirms that converged results are attained. Increasing the number of elements in the bulk material or the cohesive zone, has little impact on the simulation results. The material properties for the bulk material elements and the cohesive element are shown in Table 1.

**Table 1.** Material properties

$\sigma_y$ (Pa)	$E$ (GPa)	$\nu$	$\Gamma_0$ (N/m)	$E_{coh}$ (GPa)	$\sigma_c$ (Pa)	$\delta_c$ (m)	$\delta_1$ (m)	$\delta_2$ (m)	C
3.4e8	193	0.29	49320	17 e3	3.6e8	0.168e-3	0.02 e-3	0.126 e-3	20

The boundary conditions applied to the model are shown in Figure 7, with nodes at the lower edge fixed in all directions. The top edge is subjected to a uniform displacement in the y-direction. The load is applied in seven steps: first a ramp load that increases from zero to 5.8E-5m and then the following steps are set to have a sinusoidal load with 5.8E-5m mean displacement and amplitude of (5.8E-5, 6.2E-5, 6.5E-5, 8.6E-5, 11.2E-5, 12.6E-5, 20.6E-5m), respectively. An example of load incremental steps is shown in Figure 8.

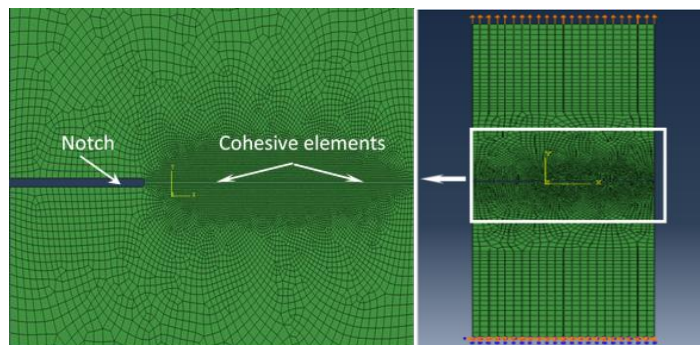


**Figure 7.** Boundary conditions and loading for FE model

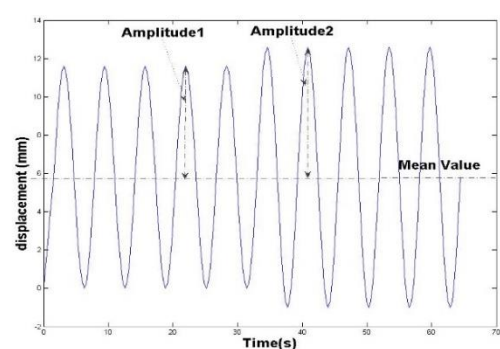


**Figure 8.** Load as function of time

The pre-cracked tension specimen is loaded in ABAQUS at four different applied frequencies (0.05, 0.1, 0.5 and 30Hz). The curves for crack length vs number of cycles for the four frequencies are shown in Figure 9. The predicted results match expectations since the model correctly predicts slower crack

propagation at higher frequency. Figure 10a and Figure 10b shows contour graphs of the finite element simulation at 0.05Hz and 30Hz respectively after 80 loading cycles.

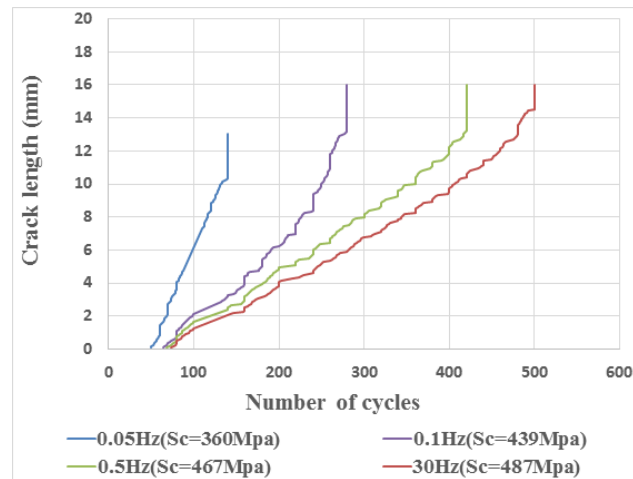


**Figure 9.** a-N curves at different frequencies

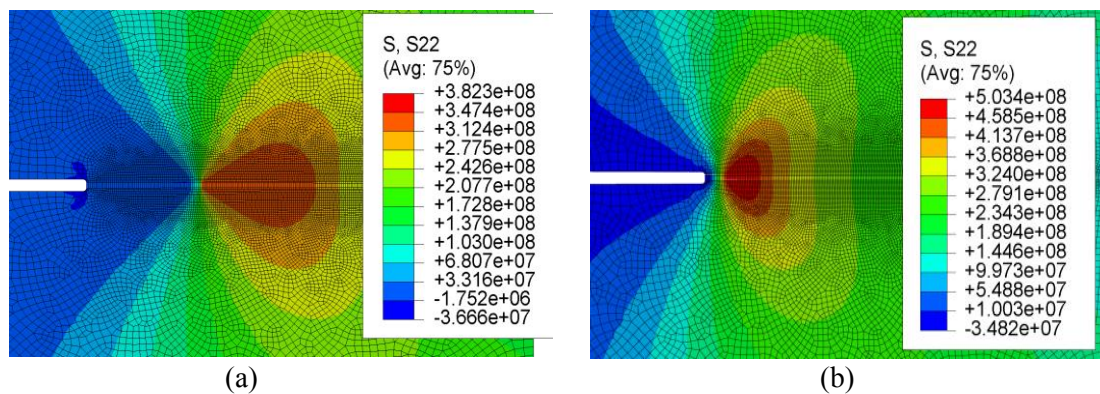


**Figure 10.** (a)Crack length after 80 cycles at 0.05Hz, (b) Crack length after 80 cycles at 30Hz

#### 4. Conclusions and future work

Based on the finding of this study the following can be concluded:

- A new CZM that combines cyclic damage with the monotonic damage has been established and applied to simulate fatigue crack propagation.
- The new CZM is founded on a rate-dependent methodology previously established by the authors, and has been shown to capture frequency effects on fatigue crack propagation in stainless steel 304.
- The new rate-dependent CZM has been implemented in the finite element solver ABAQUS (via a bespoke UMAT routine) and has been tested at different applied frequencies (0.05, 0.1, 0.5 and 30Hz).
- An experimental fatigue investigation is currently underway to validate the new cohesive model.

#### Acknowledgments

The authors would like to acknowledge the Higher Committee for Education Development in Iraq and the College of Engineering at Babylon University for providing support for Sarmed Salih to facilitate his doctoral research at the University of Manchester.

## References

- [1] J. Schijve, *Fatigue of structures and materials*. Dordrecht: Kluwer Academic Publishers, 2001.
- [2] H. Dahlan, "A Fast-Track Method for Fatigue Crack Growth Prediction with a Cohesive Zone Model," University of Manchester, 2013.
- [3] D. Dugdale, "Yielding of steel sheets containing slits," *J. Mech. Phys. Solids*, vol. 8, no. 2, pp. 100–104, 1960.
- [4] G. I. Barenblatt, "The mathematical theory of equilibrium cracks in brittle fracture," *Adv. Appl. Mech.*, vol. 7, no. 1, pp. 55–129, 1962.
- [5] I. Scheider, "Cohesive model for crack propagation analyses of structures with elastic–plastic material behavior Foundations and implementation," *GKSS Res. Cent. Geesthacht, Dept. WMS*, 2001.
- [6] A. Hillerborg, M. Mod  er, and P. Petersson, "Analysis of crack formation and crack growth in concrete by means of fracture mechanics and finite elements," *Cem. Concr. Res.*, vol. 6, pp. 773–782, 1976.
- [7] A. Needleman, "A continuum model for void nucleation by inclusion debonding," *J. Appl. Mech.*, vol. 54, no. September, pp. 525–531, 1987.
- [8] A. Needleman, "An analysis of tensile decohesion along an interface," *J. Mech. Phys. Solids*, vol. 38, no. 3, pp. 289–324, Jan. 1990.
- [9] V. Tvergaard and J. W. Hutchinson, "The relation between crack growth resistance and fracture process parameters in elastic-plastic solids," *J. Mech. Phys. Solids*, vol. 40, no. 6, pp. 1377–1397, Aug. 1992.
- [10] G. Camacho and M. Ortiz, "Computational modelling of impact damage in brittle materials," *Int. J. Solids Struct.*, vol. 33, no. 20–22, pp. 2899–2938, 1996.
- [11] G. Alfano, S. De Barros, L. Champaney, and N. Valoroso, "Comparison Between Two Cohesive-Zone Models for the Analysis of Interface Debonding," *Eur. Congr. Comput. Methods Appl. Sci. Eng.*, pp. 1–18, 2004.
- [12] P. P. Camanho, C. G. Davla, and M. F. De Moura, "Numerical simulation of mixed-mode progressive delamination in composite materials," *J. Compos. ...*, vol. 37, no. 16, 2003.
- [13] S. Salih, K. Davey, and Z. Zou, "Rate-dependent elastic and elasto-plastic cohesive zone models for dynamic crack propagation," *Int. J. Solids Struct.*, vol. 0, pp. 1–21, 2016.
- [14] A. De-Andr  s, J. P  rez, and M. Ortiz, "Elastoplastic finite element analysis of three-dimensional fatigue crack growth in aluminum shafts subjected to axial loading," *Int. J. Solids Struct.*, vol. 36, no. 15, pp. 2231–2258, 1999.
- [15] O. Nguyen and E. Repetto, "A cohesive model of fatigue crack growth," *Int. J. Fract.*, vol. 110, pp. 351–369, 2001.
- [16] K. L. Roe and T. Siegmund, "An irreversible cohesive zone model for interface fatigue crack growth simulation," *Eng. Fract. Mech.*, vol. 70, no. 2, pp. 209–232, Jan. 2003.
- [17] B. Yang, S. Mall, and K. Ravi-Chandar, "A cohesive zone model for fatigue crack growth in quasibrittle materials," *Int. J. Solids Struct.*, vol. 38, no. 22–23, pp. 3927–3944, May 2001.
- [18] P. Beaupreire and G. I. Schu  ller, "Modeling of the variability of fatigue crack growth using cohesive zone elements," *Eng. Fract. Mech.*, vol. 78, no. 12, pp. 2399–2413, Aug. 2011.
- [19] A. Ural, V. R. Krishnan, and K. D. Papoulia, "A cohesive zone model for fatigue crack growth allowing for crack retardation," *Int. J. Solids Struct.*, vol. 46, no. 11–12, pp. 2453–2462, Jun. 2009.
- [20] A. Turon, J. Costa, P. P. Camanho, and C. G. D  vila, "Simulation of delamination in composites under high-cycle fatigue," *Compos. Part A Appl. Sci. Manuf.*, vol. 38, no. 11, pp. 2270–2282, Nov. 2007.
- [21] ABAQUS, *ABAQUS 6.13 User Guide*. USA: Dassault Syst  mes Simulia Corp, 2013.